

DiffusionTalker: Personalization and Acceleration for Speech-Driven 3D Face Diffuser

Peng Chen^{1,2*}, Xiaobao Wei^{1,2*}, Ming Lu³, Yitong Zhu^{1,2},
Naiming Yao¹, Xingyu Xiao⁴, Hui Chen^{1†}

¹Institute of Software, Chinese Academy of Sciences

²University of Chinese Academy of Sciences

³Intel Labs China ⁴Tsinghua University

chenpeng23@mailsucas.ac.cn

Abstract

Speech-driven 3D facial animation has been an attractive task in both academia and industry. Traditional methods mostly focus on learning a deterministic mapping from speech to animation. Recent approaches start to consider the non-deterministic fact of speech-driven 3D face animation and employ the diffusion model for the task. However, personalizing facial animation and accelerating animation generation are still two major limitations of existing diffusion-based methods. To address the above limitations, we propose *DiffusionTalker*, a diffusion-based method that utilizes contrastive learning to personalize 3D facial animation and knowledge distillation to accelerate 3D animation generation. Specifically, to enable personalization, we introduce a learnable talking identity to aggregate knowledge in audio sequences. The proposed identity embeddings extract customized facial cues across different people in a contrastive learning manner. During inference, users can obtain personalized facial animation based on input audio, reflecting a specific talking style. With a trained diffusion model with hundreds of steps, we distill it into a lightweight model with 8 steps for acceleration. Extensive experiments are conducted to demonstrate that our method outperforms state-of-the-art methods. The code will be released.

1. Introduction

Speech-driven 3D facial animation is a crucial task in virtual reality [46], augmented reality [8] and computer gaming [10, 32, 49] applications. To achieve high-fidelity facial animation, animators need to iteratively adjust facial parameters to fit target performers. With the development of deep learning, end-to-end speech-driven facial anima-

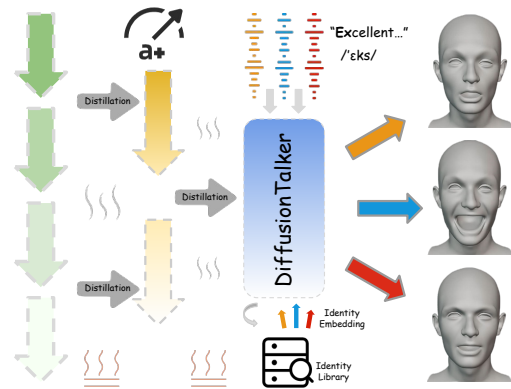


Figure 1. **DiffusionTalker**. We reduce the steps of the diffusion model for faster inference by knowledge distillation. Based on the model with fewer steps, given an audio sequence, we can find a matching identity embedding in the identity library to personalize the speaker’s talking style.

tion synthesis has been widely explored. Recent works focus on deep learning-based 3D facial animation, which can produce more vivid animation and facilitate cost reduction. Based on the convolution neural network [9, 35] or transformer [11, 30, 45], these works try to learn a mapping between audio input and mesh or blendshape [22] output. Traditional methods mainly focus on learning a deterministic mapping from speech to animation [9, 11, 30, 35]. Recently, the diffusion model has shown promising potential in learning non-deterministic mapping [16, 36, 41, 42]. In other words, when strictly controlling lip movements [40], the upper face, which has weak correlation with speech, will exhibit a greater diversity of animations. It is the inherent non-deterministic facial cues dispersed across the face.

However, recent methods still have two major limitations. First, they suffer from a prolonged inference time [30, 35, 42], which constitutes a critical limitation in terms of

*Equal Contribution.

†Corresponding Author.

engineering applications. Secondly, in real life, people can recognize a familiar person simply by listening to his voice, discerning his identity based on unique vocal characteristics without seeing his face. Therefore, different individuals exhibit distinct speaking characteristics [1, 33], indicating the importance of personalization for speech-driven 3D facial animation.

To address these issues, we propose a novel diffusion-based approach named DiffusionTalker, for producing high-quality 3D facial animations based on the user’s speaking characteristics in a short time, as shown in Fig. 1. For the personalization capacity, we introduce novel identity embeddings corresponding to the speaking characteristics of the training people. We then train the identity encoder to encode embeddings to identity features, which respond to audio features in a contrastive learning manner [34, 44]. For the synthesis acceleration, we utilize knowledge distillation [39] to distill knowledge from teacher DiffusionTalker with enormous steps to student DiffusionTalker with few steps. To leverage dense information from dense sampling steps, we obtain student DiffusionTalker with a progressive training scheme. During inference, with the voice from a new performer, DiffusionTalker first extracts features from the voice and searches for the best corresponding identity embedding. Then, all features and the noise are concatenated and sent to the GRU-based [7] talker decoder for denoising. In such an end-to-end learning pipeline, DiffusionTalker can generate high-fidelity 3D facial animation efficiently. Our main contributions are summarized as follows:

- We introduce DiffusionTalker, an end-to-end neural network for generating personalized speech-driven 3D facial animation based on Denoising Diffusion Probabilistic Model (DDPM) [16]. We first apply contrastive learning to get personalized animation, by pulling encoded audio features and learnable identity embeddings together while pushing the mismatched farther apart.
- To reduce the time cost and maintain high-fidelity generation, we utilize knowledge distillation for DiffusionTalker. After the distillation process, DiffusionTalker generates animation efficiently and obtains 65.5 times acceleration with only 8 time steps.
- Experimental results show that our DiffusionTalker outperforms the state-of-the-art methods with 0.0969 average lip error while maintaining adequate diversities.

2. Related Work

Speech-driven 3D Facial Animation. Methods for speech-driven 3D facial animation can be divided into two branches: phoneme-based methods [3] and data-driven based methods [18, 31, 43]. Phoneme-based methods, such as JALI [10, 49], come with the advantage of easy integration into other artists’ pipelines. However, they require in-

termediary representations of phonemes for co-articulation. Different from phoneme-based methods, data-driven based methods can learn the mapping between audio and facial animation automatically. VOCA [9] is the first work that uses CNN to map voice to 3D mesh. They also propose a one-hot-style embedding for a controllable output. MeshTalk [35] tries to disentangle the audio and 3D animation in a categorical latent space, but consumes longer time with less than 100ms of audio as input. FaceFormer [11] is the first work to utilize an autoregressive transformer as the model backbone and applies the attention mechanism to extract audio context features. EmoTalk [30] focuses on integrating emotion into FaceFormer for better facial animation with a cross-attention module [45]. Upon methods, all learn a deterministic mapping between audio and facial animation, while neglecting the non-deterministic nature. FaceDiffuser [42] first attempts to apply the diffusion model to the task, but lacks the ability to personalized output. To achieve personalized facial animation, DiffusionTalker utilizes contrastive learning-based identity embeddings to store personal information.

Personalization with Diffusion Model. Personalization is a crucial technique in the research field of diffusion models. One notable approach is DreamBooth [38]. This method presents a novel pathway for the personalization of text-to-image diffusion models. Given a few images of a particular subject, the pre-trained text-to-image model can be fine-tuned to associate a unique identifier with that subject. Kumari et al. [21] also find that optimizing a few parameters in diffusion models can represent new concepts of the given images. They further propose to combine multiple concepts via closed-form constrained optimization. Liu et al. [25] find that a small portion of the neurons can correspond to a particular subject. They use the statistics of network gradients to identify the neurons. Concatenating multiple clusters of concept neurons can vividly generate all related concepts in a single image. Han et al. [14] propose to fine-tune the singular values of the weight matrices, leading to a compact and efficient parameter space for personalization. In our work, we integrated the contrastive learning [34] for matching of audio and identity modalities into the diffusion model training to achieve personalization of speaking styles based on input audio.

Distillation for Diffusion Acceleration. Diffusion models have demonstrated excellent potential for content generation [5, 19, 36, 42], and outperforming GANs [12] and autoregressive models [2, 29]. However, they suffer from slow generation due to iterative denoising. Previous studies have suggested the application of knowledge distillation to improve inference speed [15]. Specifically, a faster student model can be trained to replicate the output of a pretrained teacher diffusion model. Meng et al. [26] first train a student model to mimic the outputs of a pre-trained model, followed

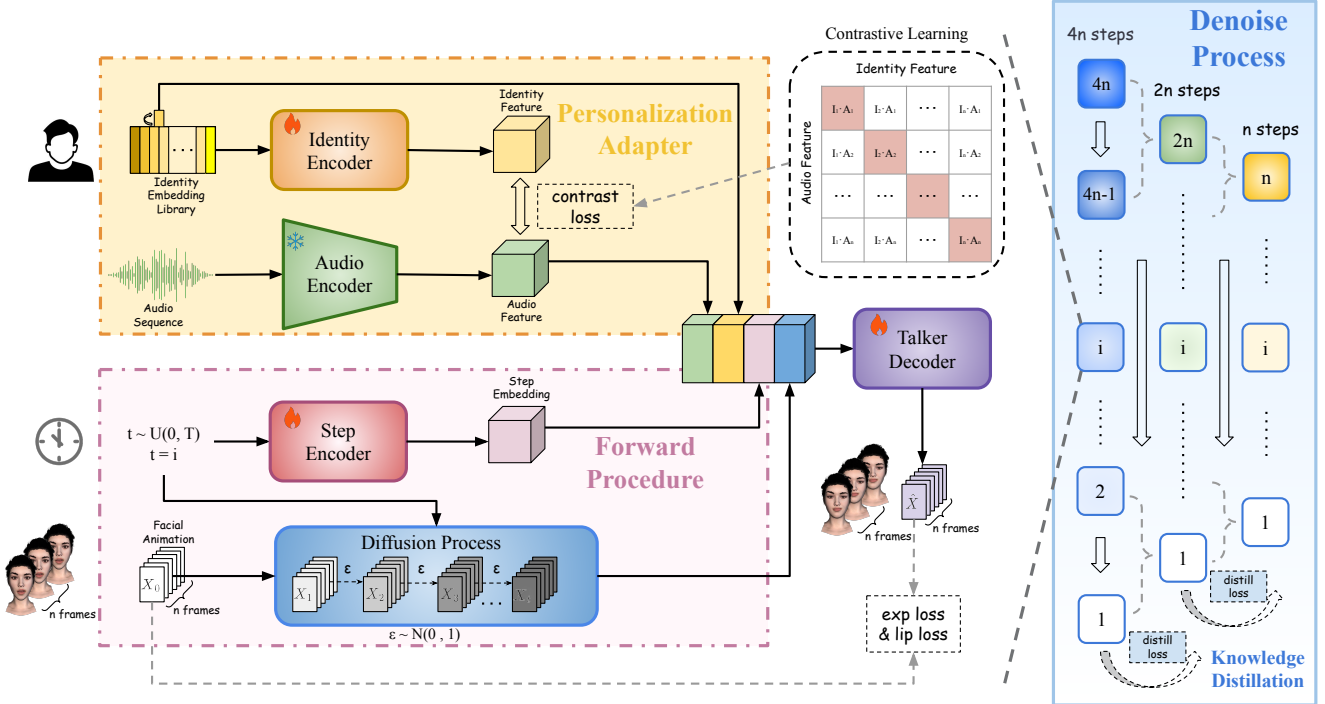


Figure 2. **Pipeline of DiffusionTalker.** DiffusionTalker continuously removes Gaussian noise from noise-added facial animation during the Denoise Process while updating the model’s parameters to generate facial animation based on input speech. In each step, the model consists of two parts: the personalization adapter, which uses contrastive learning to match speech and identity features, and the forward procedure, which adds noise to the facial parameters. Finally, all the information is fed into the talker decoder to predict facial animation. DiffusionTalker employs a training approach which is knowledge distillation and reduces the number of sampling steps by half.

by a progressive distillation. Li et al.[23] introduce an optimized UNet architecture [28, 37] that identifies and eliminates redundancies within the original model. It employs data distillation to streamline computational tasks in the image decoder and improves the efficiency of step distillation by incorporating advanced training strategies and regularization informed by classifier-free guidance. BOOT [13] circumvents the dependency on extensive offline computation using a data-free distillation algorithm, significantly enhancing the efficiency of synthetic data generation. Salimans et al. [39] propose a progressive distillation approach, halving the number of required sampling steps each time. We adopt this approach in our work, using a pre-trained large-step DiffusionTalker as a teacher model to distill a small-step student model. The aim is to accelerate the inference while also enhancing the generalization ability of the student model through knowledge distillation.

3. Methodology

In this section, we first briefly review the diffusion model. Subsequently, we proceed to elaborate on the pipeline of the proposed DiffusionTalker. Finally, we further elucidate the novel designs introduced in DiffusionTalker.

3.1. Preliminary

Denosing Diffusion Probabilistic Models (DDPMs) [16] have become a pivotal element in content generation [4, 27]. The fundamental function of DDPMs is to learn the distribution of training data and generate images that closely match this distribution. The DDPM process consists of two stages: the diffusion process and the denoise process. In the diffusion process, noise is added incrementally to the image, gradually transforming it into pure noise. The diffusion process can be characterized by a series of variance variables $\alpha_1, \alpha_2, \dots, \alpha_T$, which scale the data distribution at each step t through the diffusion sequence. The latent variable at any step t can be expressed as a function of the initial data x_0 and noise ϵ , such that:

$$x_t = \sqrt{\alpha_t}x_0 + \sqrt{1 - \alpha_t}\epsilon \quad (1)$$

where x_0 denotes the initial data distribution and x_t represents the denoised image at step t . ϵ is noise sampled from a standard Gaussian distribution $\mathcal{N}(0, I)$. $q(x_t|x_{t-1})$ is the conditional distribution of x_t given x_{t-1} , which describes the process of adding Gaussian noise to x_{t-1} , resulting in a noisier latent variable x_t at each step. The variables $\beta_1, \beta_2, \dots, \beta_T$ correspond to the noise levels added at each step of the diffusion process. These variables are related to

the variance variables through the relationships as follows.

$$\alpha_t = 1 - \beta_t \quad (2)$$

$$\bar{\alpha}_t = \alpha_1 \alpha_2 \dots \alpha_t \quad (3)$$

The denoise process is designed to reverse the diffusion process by predicting \mathbf{x}_{t-1} from \mathbf{x}_t . The goal is to approximate the true data distribution $p(\mathbf{x}_{t-1}|\mathbf{x}_t)$ starting from the noise distribution. By optimizing the parameters θ , the denoise process uses a parameterized model $p_\theta(\mathbf{x}_{t-1}|\mathbf{x}_t)$ to closely approximate the true conditional distribution $p(\mathbf{x}_{t-1}|\mathbf{x}_t)$, and ultimately, the data distribution $p(\mathbf{x})$.

During DDPM training, the objective at each step is to accurately predict the noise sampled from a Gaussian distribution. Consequently, the training loss can be formulated as follows:

$$loss = \|\epsilon - \epsilon_\theta(\sqrt{\bar{\alpha}_t}\mathbf{x}_0 + \sqrt{1 - \bar{\alpha}_t}\epsilon, t)\|^2 \quad (4)$$

where ϵ is Gaussian noise, ϵ_θ is the model that predicts t -step Gaussian noise and θ is the parameters of it.

During inference, \mathbf{x}_{t-1} can be represented as follows:

$$\mathbf{x}_{t-1} = \frac{1}{\sqrt{\alpha_t}} \left(\mathbf{x}_t - \frac{1 - \alpha_t}{\sqrt{1 - \alpha_t}} \epsilon_\theta(\mathbf{x}_t, t) \right) + \sigma_t \mathbf{z} \quad (5)$$

where $\sigma_t \mathbf{z}$ is a random noise term to generate diversity.

3.2. Overall Pipeline

DiffusionTalker is trained based on the DDPM, utilizing audio and identity as conditions to guide the denoise process of facial animation synthesis, thereby generating speech-driven 3D facial animation, as shown in Fig. 2. The specific formula employed in this process is as follows:

$$\hat{\mathbf{x}} = DiffusionTalker_\theta(\mathbf{a}, \mathbf{i}, \mathbf{x}_t, t) \quad (6)$$

where θ indicates model parameters in DiffusionTalker, \mathbf{a} is the input audio sequence, \mathbf{i} is the identity embedding from the identity embedding library, \mathbf{x}_t is \mathbf{x}_0 after t steps of the DDPM noise addition process and $\hat{\mathbf{x}}$ is the predicted facial animation which will be fitted to the ground truth \mathbf{x}_0 .

In the denoise process of DiffusionTalker, Gaussian noise is continuously removed from noise-added facial animation, and model parameters are updated to predict facial animation based on speech. Each step in this process includes two key components: the personalization adapter and the forward procedure. The former includes an identity embedding library, where each embedding corresponds to an audio sequence. The identity embedding and the audio sequence are encoded using an identity encoder and an audio encoder, respectively. Contrastive learning [6, 44, 47] is then applied to match the features of both, allowing unknown input audio to find a similar identity embedding in

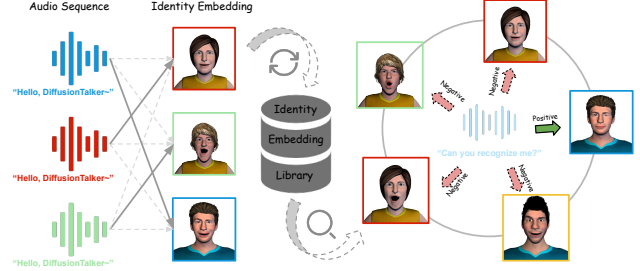


Figure 3. **Personalization Adapter.** During the training process, the personalization adapter updates the identity embedding library, whereas the inference process involves searching for the identity embedding within this library.

the identity library, thus achieving personalization of the talking style during inference. The identity embedding library can be continuously enriched and expanded by fine-tuning DiffusionTalker. The forward procedure involves the noise addition process, where Gaussian noise is added to the ground truth for t steps, with each step encoded by a step encoder. Finally, all components are fed into the talker decoder to predict facial animation parameters. To accelerate inference speed, we trained DiffusionTalker using knowledge distillation. This approach allows distilling a teacher model with $2n$ steps into a student model with n steps, accelerating the speed of speech-driven 3D face animation synthesis. We will introduce the modules in the following sections.

3.3. Personalization Adapter

To bridge the gap between audio and talking identity matching, we propose the personalization adapter by contrastive learning, ultimately achieving the personalization of identity based on speech during inference. In the personalization adapter, we have constructed an identity embedding library based on the speakers, with each speaker corresponding to an identity embedding. We have configured these embeddings as trainable parameters during the training process. Both the audio sequence and its corresponding identity embedding are fed into the network as a training pair. The former is input into a pre-trained HuBERT model [17] serving as the audio encoder to extract audio features, while the latter is received by an identity encoder with an MLP network to generate identity features. These identity embeddings and audio features are further passed on to the next layer of the network. Identity features and audio features are used to train the network with contrastive learning.

Regarding contrastive learning, we draw inspiration from [34]. However, in our approach, we have fixed the parameters of the audio encoder and only trained the identity encoder and learnable identity embeddings. The objective is to predict the correct relationship between identity embeddings and audio sequences. In terms of the specific details of contrastive learning, as shown in Fig. 3, we first

apply L2 normalization to both the identity embeddings and audio features to normalize vector lengths, preserving only directional features. Secondly, we perform matrix multiplication on the normalized representations of both, and the resulting output is used to compute the cross-entropy loss with the labels. This loss is then used to update the parameters of the personalization adapter.

During inference, a given audio sequence is input into the audio encoder, generating an audio feature. This feature is then matrix-multiplied with the features of all embeddings in the identity embedding library. The embedding with the highest similarity is identified as the talking identity matching the input audio sequence.

3.4. Knowledge Distillation

To accelerate the inference of DiffusionTalker, we utilize knowledge distillation for fewer denoise steps. Inspired by progressive distillation [39], we introduce a student model $\hat{s}_\eta(\mathbf{w}_t)$ with N steps to match the pre-trained teacher model $\hat{t}_\theta(\mathbf{w}_t)$ with $2N$ steps. \mathbf{w}_t is defined as follows:

$$\mathbf{w}_t = (\mathbf{a}, \mathbf{i}, \mathbf{x}_t, t) \quad (7)$$

where \mathbf{a} is the audio sequence, \mathbf{i} is the identity embedding corresponding to \mathbf{a} , and t is time step. We first initialize the student model with a copy of the teacher model. Then we sample data and add noise to it according to the student DDPM N steps. Before applying the student model $\hat{s}_\eta(\mathbf{w}_t)$ to denoise, we utilize the teacher model $\hat{t}_\theta(\mathbf{w}_t)$ to calculate the denoise output of $2N$ and $2N - 1$ steps. To obtain a progressive distillation, we make one student DDPM step N to match two teacher DDPM steps $2N$ and $2N - 1$.

Assume that the signal-to-noise ratio at time steps τ is $\alpha_\tau^2/\sigma_\tau^2$, then the corresponding data \mathbf{x}_0 added with noise ϵ is $\mathbf{x}_\tau = \alpha_\tau \mathbf{x}_0 + \sigma_\tau \epsilon$, $\epsilon \sim N(0, I)$. For the teacher model, we can obtain noisy data $\mathbf{x}_{\tau'}$ at time step $\tau' = 2\tau$ as the following:

$$\mathbf{x}_{\tau'} = \alpha_{\tau'} \hat{t}_\theta(\mathbf{w}_\tau) + \frac{\sigma_{\tau'}}{\sigma_\tau} (\mathbf{x}_\tau - \alpha_\tau \hat{t}_\theta(\mathbf{w}_\tau)) \quad (8)$$

For $\tau'' = 2\tau - 1$, noisy data $\mathbf{x}_{\tau''}$ can also be calculated with the above equation. As illustration in [39], the final target $\tilde{\mathbf{x}}$ from the teacher model can be formulated as:

$$\tilde{\mathbf{x}} = \frac{\mathbf{x}_{\tau''} - (\sigma_{\tau''}/\sigma_\tau) \mathbf{x}_\tau}{\alpha_{\tau''} - (\sigma_{\tau''}/\sigma_\tau) \alpha_\tau} \quad (9)$$

We apply $\tilde{\mathbf{x}}$ to supervise the student model along with other losses until convergence. Then we treat the student model with N steps as the new teacher model and repeat the same progressive knowledge distillation process. Finally, DiffusionTalker can be distilled into several steps while maintaining high-generation quality.

3.5. Training and Inference

3.5.1 Training

In our training process, we randomly select a time step t from a uniform distribution ranging from 1 to T . We then add noise to \mathbf{x}_0 for t steps to obtain \mathbf{x}_t . Audio-identity training pairs are fed into the audio encoder and the identity encoder respectively to extract features. We conduct contrastive learning between the identity feature and the audio feature. The step t is input into the step encoder to obtain a step embedding, which is then aligned with other features. Subsequently, the identity embedding, audio feature, step embedding, and \mathbf{x}_t are concatenated and input into the talker decoder for denoising, producing $\hat{\mathbf{x}}$. The model parameters are optimized based on the L2 loss between $\hat{\mathbf{x}}$ and \mathbf{x}_0 . The trainable components of this process include the identity embeddings, identity encoder, step encoder, and talker decoder, while the parameters of the audio encoder remain fixed. We propose five types of loss functions, namely, expression loss, lip loss, contrast loss, velocity loss, and distillation loss, each specifically targeted toward different constraint objectives.

During the training process of the teacher model, the overall loss is formulated as:

$$L_{tea} = \lambda_1 L_{exp} + \lambda_2 L_{lip} + \lambda_3 L_{con} + \lambda_4 L_{vel} \quad (10)$$

During the knowledge distillation process of the student model, the overall loss is formulated as:

$$L_{stu} = L_{tea} + \lambda_5 L_{dis} \quad (11)$$

where $\lambda_1 = 1.0$, $\lambda_2 = 1.0$, $\lambda_3 = 0.007$, $\lambda_4 = 0.5$, $\lambda_5 = 0.1$ are fixed in all our experiments. The formulation of these loss functions will be explained below:

Expression Loss. Expression loss is a constraint applied to all facial parameters, and its definition is as follows:

$$L_{exp} = \|\hat{\mathbf{x}} - \mathbf{x}_0\|^2 \quad (12)$$

where $\hat{\mathbf{x}}$ is the prediction of facial parameters, \mathbf{x}_0 is the ground truth of animation.

Lip Loss. In order to improve the accuracy of lip movement, we selected parameters related to the lips and applied lip loss to constrain these parameters.

$$L_{lip} = \|\hat{\mathbf{x}}' - \mathbf{x}'_0\|^2 \quad (13)$$

where $\hat{\mathbf{x}}'$ is the predicted parameters of lip area, \mathbf{x}'_0 is the label of lip animation.

Contrast Loss. Contrast loss, as a target function for contrastive learning, is utilized to achieve the personalization of the talking identity. Its definition is as follows:

$$L_{con} = -\frac{1}{M} \sum_{i=1}^M \log \frac{\sum_{t=0}^m e^{h_i^\top h_t / \tau}}{\sum_{j=0}^M e^{h_i^\top h_j / \tau}}, \quad (14)$$

where h denotes the samples involved in contrastive learning, M is the number of samples, m is the number of positive samples corresponding to i^{th} sample h_i , and τ is a temperature hyper-parameter.

Velocity Loss. We add the velocity loss from EmoTalk to enhance the smoothness between predicted animation frames. It is defined as follows:

$$L_{vel} = \sum_{i=2}^n \|(\hat{\mathbf{f}}^i - \hat{\mathbf{f}}^{i-1}) - (\mathbf{f}_0^i - \mathbf{f}_0^{i-1})\|^2 \quad (15)$$

where n is the number of total animation frames, and \mathbf{f} is the animation parameters for a single frame.

Distill Loss. We employ distill loss as the objective function for knowledge distillation, and its definition is as follows:

$$L_{dis} = \max\left(\frac{\alpha_\tau^2}{\sigma_\tau}, 1\right) \|\tilde{\mathbf{x}} - \hat{s}_\eta(\mathbf{w}_\tau)\|^2 \quad (16)$$

3.5.2 Inference

During the inference process, an input audio sequence will find its matched identity embedding in the personalization adapter, which serves as the talking identity. This embedding, along with the audio feature and other intermediate features, is concatenated and input into the talker decoder for denoising. After N steps of denoising, the final facial parameters are predicted. This process, due to the inclusion of the talking identity, achieves user personalization.

4. Experiments

4.1. Experimental Settings

Datasets. In the field of speech-driven 3D facial animation, the two most common approaches are blendshape-based facial animation [22] and vertex-based facial animation. Correspondingly, the datasets used are also categorized into blendshape-based and vertex-based datasets. Motivated by the objective of speed enhancement in DiffusionTalker, we trained our DiffusionTalker on the blendshape-based BEAT dataset [24] for its fewer parameters. BEAT are collected by Apple ARKit with 52 blendshape coefficients. It consists of voice recordings and corresponding blendshape-based facial animations from 30 different individuals. Each person says the same content but with their unique speaking style. We utilize a subset with about 32 hours of audio data from the full dataset. We further segmented the audio data into 11,427 sequences, each with a duration of 10 seconds. We follow the data preprocessing in FaceDiffuser [42].

We also employed VOCASET [9] as a zero-shot test set to more effectively evaluate the robustness of DiffusionTalker. VOCASET, a vertex-based dataset, comprises 480 facial animation sequences and the corresponding speech data, featuring 12 subjects. Each facial animation sequence consists of 5,023 vertices, multiplied by 3 to

represent spatial coordinates in the x , y , and z dimensions. The duration of each speech data segment is approximately 3-4 seconds. For testing, we adopted the Blendshape conversion method from EmoTalk [30], enabling the transformation of VOCASET into 52 blendshape coefficients.

Implementation Details. We follow the implementation details specified in FaceDiffuser [42]. For model architectures, we utilize the pretrained HuBERT [17] as an audio encoder to extract audio features. The dimension of identity embeddings is set to 32 and is sent to the identity encoder. We further concatenate the encoded features and employ a two-layer GRU. The dimension of the hidden layer is set as 256. To train the whole pipeline, we utilize the Adam optimizer [20] with $(\beta_1, \beta_2) = (0.9, 0.999)$ to update parameters, and the learning rate is set to $1e^{-4}$. We set a linear β schedule for 32 steps for teacher models. We first train the teacher model with 50 epochs. Then we copy the weights of the teacher model into the student model and apply the proposed knowledge distillation techniques to train the student model with half-time steps. We iteratively set the student model as the teacher model to further reduce sampling time steps. All experiments are conducted on NVIDIA V100 GPUs. More implementation details are reported in the supplementary material.

Evaluation Metrics. To quantitatively assess the performance and robustness of DiffusionTalker, we employed four key evaluation metrics: MBE, LBE, FDD, and ITF.

(MBE) Mean Blendshape Error measures the average Euclidean distance between the predicted blendshape coefficients and the ground truth. Lower MBE values indicate higher accuracy, as they represent smaller deviations from the ground truth.

(LBE) Lip Blendshape Error measures the discrepancy between the predicted and ground truth blendshape coefficients associated with the lip region.

(FDD) Facial Dynamics Deviation [48] measures the deviation in the dynamics of the upper face region between the generated sequence and the ground truth.

(ITF) Inference Time per Frame is defined as the inference time per audio frame, calculated by dividing the total inference time by the total number of audio frames. This metric is employed to quantitatively measure and compare the inference speed of models.

4.2. Experimental Results

4.2.1 Quantitative Evaluation

We trained six DiffusionTalker models from scratch on the BEAT dataset, with steps set covering 256, 128, 64, 32, 16, and 8 respectively. Subsequently, we employed the knowledge distillation approach where a 32-step model served as the teacher model to train a 16-step student model. This 16-step student model was then used as a new teacher to distill an 8-step student model.

Table 1. **The performance and inference speed of our model vary with different step counts.** Specifically, the inference speed of the 8-step model is enhanced when using NVIDIA TensorRT.

Dataset	Steps	Distilled	LBE↓	FDD ↓	ITF(10^{-4} s)↓
BEAT	256	✗	0.1050	0.1693	255.5
	128	✗	0.1059	0.1445	132.4
	64	✗	0.1063	0.1517	65.3
	32	✗	0.1053	0.1647	32.2
	16	✗	0.1097	0.1656	16.8
	8	✗	0.1177	0.1709	7.0
	16	✓	0.0957	0.1433	16.8
	8	✓	0.0969	0.1558	7.1
	8(TRT)	✓	0.0975	0.1563	3.9

Table 2. **The quantitative results evaluated on the 3D blendshape dataset.** Various models were tested on the BEAT dataset, with the best results highlighted in bold. Among them, FaceDiffuser is a 1000-step model. Our model demonstrates superior performance in MBE, LBE, and ITF, except for the FDD metric.

Dataset	Method	MBE ↓	LBE ↓	FDD ↓	ITF(10^{-4} s)↓
BEAT	EmoTalk	1.0537	0.2628	0.0751	9.3
	FaceDiffuser	0.4332	0.1071	0.1786	1000.9
	FaceDiffuser-8	0.8372	0.2115	0.0589	8.2
	Ours-8	0.4094	0.0969	0.1558	7.1

In our quantitative experiments, we conduct three sets of tests. In the first set, we assess and compare the performance metrics of all nine models, ranging from 256 to 8 steps. In the second set, we retrain FaceDiffuser on the BEAT dataset. EmoTalk, FaceDiffuser, and the 8-step distilled DiffusionTalker are tested on BEAT, and metrics such as MBE, LBE, FDD, and ITF are reported. The reason for selecting EmoTalk and FaceDiffuser as baselines is that other methods do not release the training code on blendshape-based datasets. In the third set, we retrain FaceDiffuser on the VOCASET and conduct an evaluation. We use the test results from EmoTalk’s paper, including methods like FaceFormer and EmoTalk on VOCASET. Our 8-step distilled DiffusionTalker trained on BEAT is directly tested on VOCASET and compared with other methods. In the third set, We focus on lip accuracy and inference time, hence the LVE and ITF metrics are reported.

Inference Speed. As shown in Tab. 1, the ITF decreases as the number of steps reduces, indicating that a decrease in steps leads to an increase in the inference speed. This observation aligns with our general understanding. Consequently, we plotted ITF against the number of steps, as depicted in Fig. 4, which demonstrates a direct proportional relationship between ITF and steps, further indicating an inverse relationship between model inference speed and the number of steps. The last row of Tab. 1 highlights that upon integrating the 8-step distilled model with NVIDIA TensorRT, the ITF decreased from 7.1×10^{-4} s to 3.9×10^{-4} s,

Table 3. **The quantitative results evaluated on the 3D vertex dataset.** Various models were tested on the VOCASET dataset, with the best results highlighted in bold. Our model, without being trained on the VOCASET dataset, demonstrated optimal performance in terms of the LVE and ITF metrics under the zero-shot condition.

Dataset	Method	LVE ↓	ITF(10^{-4} s)↓	Zero-Shot
VOCASET	FaceFormer	4.418	54.2	✗
	EmoTalk	4.413	9.3	✓
	FaceDiffuser-8	4.713	8.2	✗
	Ours-8	1.607	7.1	✓

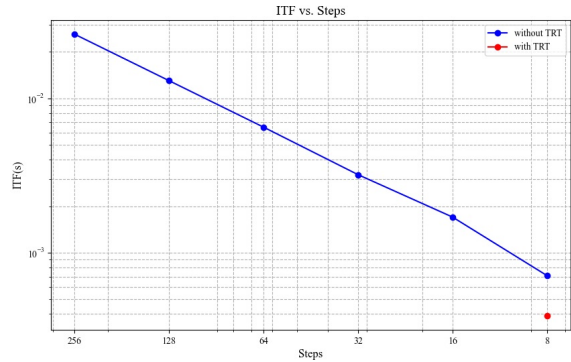


Figure 4. **ITF vs. Steps.** The inference speeds of the model with and without NVIDIA TensorRT vary under different step counts.

resulting in an 82.1% increase in inference speed.

We compared the 8-step distilled model on the BEAT and VOCASET test sets with other methods, as illustrated in Tab. 2 and 3. The model exhibited the best ITF metric in both cases, indicating the fastest inference speed. Our method achieves a similar speed compared with FaceDiffuser-8, however, our quantitative results are much better thanks to the personalization ability.

Fidelity and Accuracy. Lip movement precision is a crucial factor for evaluating fidelity and accuracy in the speech-driven 3D facial animation field. As indicated in Tab. 1, without knowledge distillation, the LBE and FDD metrics slightly increase as the number of steps decreases. This suggests that reducing the steps in a diffusion model can lead to a decrease in accuracy. During the transition from 16 to 8 steps with knowledge distillation, this trend persists. However, models obtained through knowledge distillation at identical step counts (16 or 8) significantly outperform their non-distilled counterparts in terms of LBE and FDD. This implies that models derived via knowledge distillation exhibit enhanced accuracy. This trend can be attributed to (1) a reduction in the model’s steps, leading to fewer sampling steps and potentially inadequate de-noising, affecting precision; (2) during knowledge distillation, the student model learns soft labels from the teacher model, encompassing the latter’s understanding of the data, which might

Table 4. **Identity matching results.**

Metrics	Precision	Recall	F1 Score
Results(%)	99.996	99.986	99.991

Table 5. **Ablation study for our 8-step model.** We conducted an evaluation of key components within our model by assessing the impact on MBE and LBE metrics in their absence.

Ablation Settings	MBE↓	LBE ↓
Ours	0.4094	0.0969
w/o knowledge distillation	0.4545	0.1177
w/o L_{lip} loss	0.4222	0.1037
w/o L_{vel} loss	0.4414	0.1129
w/o identity embedding	0.4306	0.1034

aid the student model in better generalizing to unseen data; (3) using the soft outputs of the teacher model as targets may provide a regularizing effect, helping to prevent overfitting in the student model.

Tab. 2 and 3 demonstrate that our approach achieves state-of-the-art performance in MBE and LBE metrics, both on BEAT and VOCASET. However, our model exhibits suboptimal performance in the FDD metric. This suggests a weaker inference capability in terms of facial dynamics deviation, particularly in the upper face region. This limitation could stem from the model’s excessive focus on lip accuracy constraints, leading to a comparatively lesser emphasis on dynamics of areas with weak correlation to speech.

Identity Matching. Identity matching is a crucial component for achieving personalization ability. We tested our 8-step distilled model on the whole BEAT dataset. As shown in Tab. 4, the results indicate that our contrastive learning approach effectively integrates the audio and identity modalities, achieving high accuracy in identity matching.

Effectiveness of Each Component. We conducted a study to evaluate the impact of each component. As presented in Tab. 5, both metrics increase without knowledge distillation. The L_{lip} loss specifically reduces the error rate in the lip region, while the L_{vel} loss focuses on the differences in overall blendshapes between frames. The absence of identity embedding could lead to a decrease in performance. This study shows the effectiveness of each component.

4.2.2 Qualitative Evaluation

Talking Identity Personalization. As shown in Fig. 5, we choose five audio sequences from different people. For instance, Person 1 consistently speaks with exaggerated facial expressions, displaying larger facial movement amplitudes. Compared with other methods, DiffusionTalker generates facial animations that are closer to the ground truth, effec-

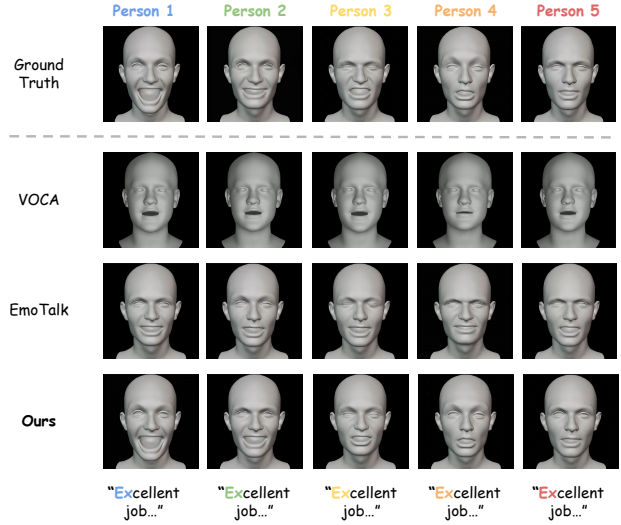


Figure 5. **Qualitative comparisons on various talking identities with other methods.** We selected audio sequences from five different individuals as tests. In each of the cases representing different talking identities, we emitted the $/\text{'εks}/$ sound in the word "excellent." We conducted qualitative comparisons with ground truth respectively using VOCA, EmoTalk, and DiffusionTalker.

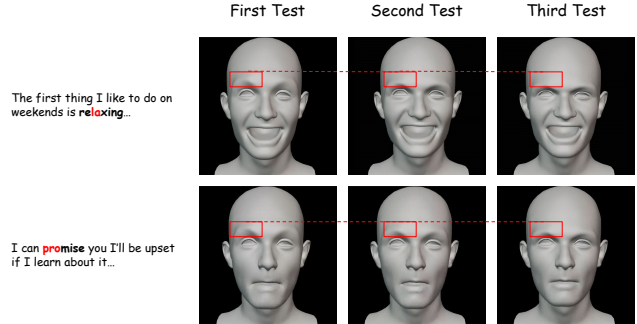


Figure 6. **Facial Expression Diversity.** The location of eyebrows is non-deterministic among various tests.

tively demonstrating the personal talking identity. On the other hand, VOCA and EmoTalk are less proficient in this regard, failing to capture and display the unique speaking expression habits and styles of individuals. The qualitative comparisons tested on VOCASET and user study are reported in the supplementary materials.

Facial Expression Diversity. As illustrated in Fig. 6. Under the same input audio and identity, we conducted three inferences. It can be observed that, in the same audio frame, the corresponding animation frames show noticeable differences in the position of the eyebrows, demonstrating the non-deterministic fact of speech-driven 3D face animation.

5. Conclusion

To generate personalized speech-driven 3D facial animation in a short time, we propose a diffusion-based method named

DiffusionTalker. The paper applies contrastive learning between encoded audio features and learnable talking identity to aggregate personal information. To further accelerate the inference time, we distill dense knowledge from a teacher model with huge sampling steps into a student model with much fewer sampling steps while maintaining competitive accuracy. Finally, we conduct detailed experiments on two datasets BEAT and VOCASET, demonstrating the effectiveness of our proposed method. In the future, we will explore more natural 3D facial animation, and personalized facial texture features based on speech show promising potential.

References

- [1] Joan A Argente. From speech to speaking styles. *Speech communication*, 11(4-5):325–335, 1992. 2
- [2] Tom Brown, Benjamin Mann, Nick Ryder, Melanie Subbiah, Jared D Kaplan, Prafulla Dhariwal, Arvind Neelakantan, Pranav Shyam, Girish Sastry, Amanda Askell, et al. Language models are few-shot learners. *Advances in neural information processing systems*, 33:1877–1901, 2020. 2
- [3] Constantinos Charalambous, Zerrin Yumak, and A Frank van der Stappen. Audio-driven emotional speech animation for interactive virtual characters. *Computer Animation and Virtual Worlds*, 30(3-4):e1892, 2019. 2
- [4] Nanxin Chen, Yu Zhang, Heiga Zen, Ron J Weiss, Mohammad Norouzi, and William Chan. Wavegrad: Estimating gradients for waveform generation. *arXiv preprint arXiv:2009.00713*, 2020. 3
- [5] Shoufa Chen, Peize Sun, Yibing Song, and Ping Luo. Diffusiondet: Diffusion model for object detection. In *Proceedings of the IEEE/CVF International Conference on Computer Vision*, pages 19830–19843, 2023. 2
- [6] Ting Chen, Simon Kornblith, Mohammad Norouzi, and Geoffrey Hinton. A simple framework for contrastive learning of visual representations. In *International conference on machine learning*, pages 1597–1607. PMLR, 2020. 4
- [7] Kyunghyun Cho, Bart Van Merriënboer, Caglar Gulcehre, Dzmitry Bahdanau, Fethi Bougares, Holger Schwenk, and Yoshua Bengio. Learning phrase representations using rnn encoder-decoder for statistical machine translation. *arXiv preprint arXiv:1406.1078*, 2014. 2
- [8] Gérard Chollet, Anna Esposito, Annie Gentes, Patrick Hoirain, Walid Karam, Zhenbo Li, Catherine Pelachaud, Patrick Perrot, Dijana Petrovska-Delacrétaz, Dianle Zhou, et al. Multimodal human machine interactions in virtual and augmented reality. *Multimodal Signals: Cognitive and Algorithmic Issues: COST Action 2102 and euCognition International School Vietri sul Mare, Italy, April 21-26, 2008 Revised Selected and Invited Papers*, pages 1–23, 2009. 1
- [9] Daniel Cudeiro, Timo Bolkart, Cassidy Laidlaw, Anurag Ranjan, and Michael J Black. Capture, learning, and synthesis of 3d speaking styles. In *Proceedings of the IEEE/CVF Conference on Computer Vision and Pattern Recognition*, pages 10101–10111, 2019. 1, 2, 6
- [10] Pif Edwards, Chris Landreth, Eugene Fiume, and Karan Singh. Jali: an animator-centric viseme model for expressive lip synchronization. *ACM Transactions on graphics (TOG)*, 35(4):1–11, 2016. 1, 2
- [11] Yingruo Fan, Zhaojiang Lin, Jun Saito, Wenping Wang, and Taku Komura. Faceformer: Speech-driven 3d facial animation with transformers. In *Proceedings of the IEEE/CVF Conference on Computer Vision and Pattern Recognition*, pages 18770–18780, 2022. 1, 2
- [12] Ian Goodfellow, Jean Pouget-Abadie, Mehdi Mirza, Bing Xu, David Warde-Farley, Sherjil Ozair, Aaron Courville, and Yoshua Bengio. Generative adversarial nets. *Advances in neural information processing systems*, 27, 2014. 2
- [13] Jiatao Gu, Shuangfei Zhai, Yizhe Zhang, Lingjie Liu, and Joshua M Susskind. Boot: Data-free distillation of denoising diffusion models with bootstrapping. In *ICML 2023 Workshop on Structured Probabilistic Inference* {\&} *Generative Modeling*, 2023. 3
- [14] Ligong Han, Yinxiao Li, Han Zhang, Peyman Milanfar, Dimitris Metaxas, and Feng Yang. Svdiff: Compact parameter space for diffusion fine-tuning. *arXiv preprint arXiv:2303.11305*, 2023. 2
- [15] Geoffrey Hinton, Oriol Vinyals, and Jeff Dean. Distilling the knowledge in a neural network. *arXiv preprint arXiv:1503.02531*, 2015. 2
- [16] Jonathan Ho, Ajay Jain, and Pieter Abbeel. Denoising diffusion probabilistic models. *Advances in neural information processing systems*, 33:6840–6851, 2020. 1, 2, 3
- [17] Wei-Ning Hsu, Benjamin Bolte, Yao-Hung Hubert Tsai, Kushal Lakhotia, Ruslan Salakhutdinov, and Abdelrahman Mohamed. Hubert: Self-supervised speech representation learning by masked prediction of hidden units. *IEEE/ACM Transactions on Audio, Speech, and Language Processing*, 29:3451–3460, 2021. 4, 6
- [18] Dong-Yan Huang, Ellensi Chandra, Xiangting Yang, Ying Zhou, Huaiping Ming, Weisi Lin, Minghui Dong, and Haizhou Li. Visual speech emotion conversion using deep learning for 3d talking head. In *Proceedings of the Joint Workshop of the 4th Workshop on Affective Social Multimedia Computing and first Multi-Modal Affective Computing of Large-Scale Multimedia Data*, pages 7–13, 2018. 2
- [19] Yuanfeng Ji, Zhe Chen, Enze Xie, Lanqing Hong, Xihui Liu, Zhaoqiang Liu, Tong Lu, Zhenguo Li, and Ping Luo. Ddp: Diffusion model for dense visual prediction. *arXiv preprint arXiv:2303.17559*, 2023. 2
- [20] Diederik P Kingma and Jimmy Ba. Adam: A method for stochastic optimization. *arXiv preprint arXiv:1412.6980*, 2014. 6
- [21] Nupur Kumari, Bingliang Zhang, Richard Zhang, Eli Shechtman, and Jun-Yan Zhu. Multi-concept customization of text-to-image diffusion. In *Proceedings of the IEEE/CVF Conference on Computer Vision and Pattern Recognition*, pages 1931–1941, 2023. 2
- [22] John P Lewis, Ken Anjyo, Taehyun Rhee, Mengjie Zhang, Frederic H Pighin, and Zhigang Deng. Practice and theory of blendshape facial models. *Eurographics (State of the Art Reports)*, 1(8):2, 2014. 1, 6
- [23] Yanyu Li, Huan Wang, Qing Jin, Ju Hu, Pavlo Chemerys, Yun Fu, Yanzhi Wang, Sergey Tulyakov, and Jian Ren. Snapfusion: Text-to-image diffusion model on mobile devices

- within two seconds. *arXiv preprint arXiv:2306.00980*, 2023. [3](#)
- [24] Haiyang Liu, Zihao Zhu, Naoya Iwamoto, Yichen Peng, Zhengqing Li, You Zhou, Elif Bozkurt, and Bo Zheng. Beat: A large-scale semantic and emotional multi-modal dataset for conversational gestures synthesis. In *Computer Vision – ECCV 2022: 17th European Conference, Tel Aviv, Israel, October 23–27, 2022, Proceedings, Part VII*, page 612–630, Berlin, Heidelberg, 2022. Springer-Verlag. [6](#)
- [25] Zhiheng Liu, Ruili Feng, Kai Zhu, Yifei Zhang, Kecheng Zheng, Yu Liu, Deli Zhao, Jingren Zhou, and Yang Cao. Cones: Concept neurons in diffusion models for customized generation. *arXiv preprint arXiv:2303.05125*, 2023. [2](#)
- [26] Chenlin Meng, Robin Rombach, Ruiqi Gao, Diederik Kingma, Stefano Ermon, Jonathan Ho, and Tim Salimans. On distillation of guided diffusion models. In *Proceedings of the IEEE/CVF Conference on Computer Vision and Pattern Recognition*, pages 14297–14306, 2023. [2](#)
- [27] Alex Nichol, Prafulla Dhariwal, Aditya Ramesh, Pranav Shyam, Pamela Mishkin, Bob McGrew, Ilya Sutskever, and Mark Chen. Glide: Towards photorealistic image generation and editing with text-guided diffusion models. *arXiv preprint arXiv:2112.10741*, 2021. [3](#)
- [28] Ozan Oktay, Jo Schlemper, Loic Le Folgoc, Matthew Lee, Matthias Heinrich, Kazunari Misawa, Kensaku Mori, Steven McDonagh, Nils Y Hammerla, Bernhard Kainz, et al. Attention u-net: Learning where to look for the pancreas. *arXiv preprint arXiv:1804.03999*, 2018. [3](#)
- [29] Aaron van den Oord, Sander Dieleman, Heiga Zen, Karen Simonyan, Oriol Vinyals, Alex Graves, Nal Kalchbrenner, Andrew Senior, and Koray Kavukcuoglu. Wavenet: A generative model for raw audio. *arXiv preprint arXiv:1609.03499*, 2016. [2](#)
- [30] Ziqiao Peng, Haoyu Wu, Zhenbo Song, Hao Xu, Xiangyu Zhu, Jun He, Hongyan Liu, and Zhaoxin Fan. Emotalk: Speech-driven emotional disentanglement for 3d face animation. In *Proceedings of the IEEE/CVF International Conference on Computer Vision*, pages 20687–20697, 2023. [1](#), [2](#), [6](#)
- [31] Hai Xuan Pham, Yuting Wang, and Vladimir Pavlovic. End-to-end learning for 3d facial animation from speech. In *Proceedings of the 20th ACM International Conference on Multimodal Interaction*, pages 361–365, 2018. [2](#)
- [32] Heng Yu Ping, Lili Nurliyana Abdullah, Puteri Suhaiza Sulaiman, and Alfian Abdul Halin. Computer facial animation: A review. *International Journal of Computer Theory and Engineering*, 5(4):658, 2013. [1](#)
- [33] KR Prajwal, Rudrabha Mukhopadhyay, Vinay P Namboodiri, and CV Jawahar. Learning individual speaking styles for accurate lip to speech synthesis. In *Proceedings of the IEEE/CVF Conference on Computer Vision and Pattern Recognition*, pages 13796–13805, 2020. [2](#)
- [34] Alec Radford, Jong Wook Kim, Chris Hallacy, Aditya Ramesh, Gabriel Goh, Sandhini Agarwal, Girish Sastry, Amanda Askell, Pamela Mishkin, Jack Clark, et al. Learning transferable visual models from natural language supervision. In *International conference on machine learning*, pages 8748–8763. PMLR, 2021. [2](#), [4](#)
- [35] Alexander Richard, Michael Zollhöfer, Yandong Wen, Fernando De la Torre, and Yaser Sheikh. Meshtalk: 3d face animation from speech using cross-modality disentanglement. In *Proceedings of the IEEE/CVF International Conference on Computer Vision*, pages 1173–1182, 2021. [1](#), [2](#)
- [36] Robin Rombach, Andreas Blattmann, Dominik Lorenz, Patrick Esser, and Björn Ommer. High-resolution image synthesis with latent diffusion models. In *Proceedings of the IEEE/CVF conference on computer vision and pattern recognition*, pages 10684–10695, 2022. [1](#), [2](#)
- [37] Olaf Ronneberger, Philipp Fischer, and Thomas Brox. U-net: Convolutional networks for biomedical image segmentation. In *Medical Image Computing and Computer-Assisted Intervention–MICCAI 2015: 18th International Conference, Munich, Germany, October 5-9, 2015, Proceedings, Part III 18*, pages 234–241. Springer, 2015. [3](#)
- [38] Nataniel Ruiz, Yuanzhen Li, Varun Jampani, Yael Pritch, Michael Rubinstein, and Kfir Aberman. Dreambooth: Fine tuning text-to-image diffusion models for subject-driven generation. In *Proceedings of the IEEE/CVF Conference on Computer Vision and Pattern Recognition*, pages 22500–22510, 2023. [2](#)
- [39] Tim Salimans and Jonathan Ho. Progressive distillation for fast sampling of diffusion models. *arXiv preprint arXiv:2202.00512*, 2022. [2](#), [3](#), [5](#)
- [40] Changchong Sheng, Gangyao Kuang, Liang Bai, Chenping Hou, Yulan Guo, Xin Xu, Matti Pietikäinen, and Li Liu. Deep learning for visual speech analysis: A survey. *arXiv preprint arXiv:2205.10839*, 2022. [1](#)
- [41] Jiaming Song, Chenlin Meng, and Stefano Ermon. Denoising diffusion implicit models. *arXiv preprint arXiv:2010.02502*, 2020. [1](#)
- [42] Stefan Stan, Kazi Injamamul Haque, and Zerrin Yumak. Facediffuser: Speech-driven 3d facial animation synthesis using diffusion. *arXiv preprint arXiv:2309.11306*, 2023. [1](#), [2](#), [6](#)
- [43] Sarah Taylor, Taehwan Kim, Yisong Yue, Moshe Mahler, James Krahe, Anastasio Garcia Rodriguez, Jessica Hodgins, and Iain Matthews. A deep learning approach for generalized speech animation. *ACM Transactions On Graphics (TOG)*, 36(4):1–11, 2017. [2](#)
- [44] Yonglong Tian, Dilip Krishnan, and Phillip Isola. Contrastive multiview coding. In *Computer Vision–ECCV 2020: 16th European Conference, Glasgow, UK, August 23–28, 2020, Proceedings, Part XI 16*, pages 776–794. Springer, 2020. [2](#), [4](#)
- [45] Ashish Vaswani, Noam Shazeer, Niki Parmar, Jakob Uszkoreit, Llion Jones, Aidan N Gomez, Łukasz Kaiser, and Illia Polosukhin. Attention is all you need. *Advances in neural information processing systems*, 30, 2017. [1](#), [2](#)
- [46] Isabell Wohlgenannt, Alexander Simons, and Stefan Stieglitz. Virtual reality. *Business & Information Systems Engineering*, 62:455–461, 2020. [1](#)
- [47] Zhirong Wu, Yuanjun Xiong, Stella X Yu, and Dahua Lin. Unsupervised feature learning via non-parametric instance discrimination. In *Proceedings of the IEEE conference on computer vision and pattern recognition*, pages 3733–3742, 2018. [4](#)

- [48] Jinbo Xing, Menghan Xia, Yuechen Zhang, Xiaodong Cun, Jue Wang, and Tien-Tsin Wong. Codetalker: Speech-driven 3d facial animation with discrete motion prior. In *Proceedings of the IEEE/CVF Conference on Computer Vision and Pattern Recognition*, pages 12780–12790, 2023. 6
- [49] Yang Zhou, Zhan Xu, Chris Landreth, Evangelos Kalogerakis, Subhransu Maji, and Karan Singh. Visemenet: Audio-driven animator-centric speech animation. *ACM Transactions on Graphics (TOG)*, 37(4):1–10, 2018. 1, 2